

<b>Impact Factor:</b>	<b>ISRA (India) = 6.317</b>	<b>SIS (USA) = 0.912</b>	<b>ICV (Poland) = 6.630</b>
	<b>ISI (Dubai, UAE) = 1.582</b>	<b>РИНЦ (Russia) = 3.939</b>	<b>PIF (India) = 1.940</b>
	<b>GIF (Australia) = 0.564</b>	<b>ESJI (KZ) = 9.035</b>	<b>IBI (India) = 4.260</b>
	<b>JIF = 1.500</b>	<b>SJIF (Morocco) = 7.184</b>	<b>OAJI (USA) = 0.350</b>

SOI: [1.1/TAS](#) DOI: [10.15863/TAS](#)

**International Scientific Journal  
Theoretical & Applied Science**

p-ISSN: 2308-4944 (print) e-ISSN: 2409-0085 (online)

Year: 2022 Issue: 02 Volume: 106

Published: 07.02.2022 <http://T-Science.org>

QR – Issue



QR – Article



**Denis Chemezov**

Vladimir Industrial College

M.Sc.Eng., Corresponding Member of International Academy of Theoretical and Applied Sciences, Lecturer, Russian Federation

<https://orcid.org/0000-0002-2747-552X>

[vic-science@yandex.ru](mailto:vic-science@yandex.ru)

**Irina Pavlukhina**

Vladimir Industrial College

Lecturer, Russian Federation

**Daniil Kozin**

Vladimir Industrial College

Student, Russian Federation

**Vyacheslav Matveev**

Vladimir Industrial College

Student, Russian Federation

**Denis Kosolapov**

Vladimir Industrial College

Student, Russian Federation

**Sergey Prokopenko**

Vladimir Industrial College

Student, Russian Federation

**Dmitriy Smirnov**

Vladimir Industrial College

Student, Russian Federation

## REFERENCE DATA OF PRESSURE DISTRIBUTION ON THE SURFACES OF AIRFOILS HAVING THE NAMES BEGINNING WITH THE LETTER F

**Abstract:** The results of the computer calculation of air flow around the airfoils having the names beginning with the letter F are presented in the article. The contours of pressure distribution on the surfaces of the airfoils at the angles of attack of 0, 15 and -15 degrees in conditions of the subsonic airplane flight speed were obtained.

**Key words:** the airfoil, the angle of attack, pressure, the surface.

**Language:** English

**Citation:** Chemezov, D., et al. (2022). Reference data of pressure distribution on the surfaces of airfoils having the names beginning with the letter F. *ISJ Theoretical & Applied Science*, 02 (106), 101-135.

**Doi:** <http://s-o-i.org/1.1/TAS-02-106-14> **Scopus ASCC:** 1507.

<https://doi.org/10.15863/TAS.2022.02.106.14>



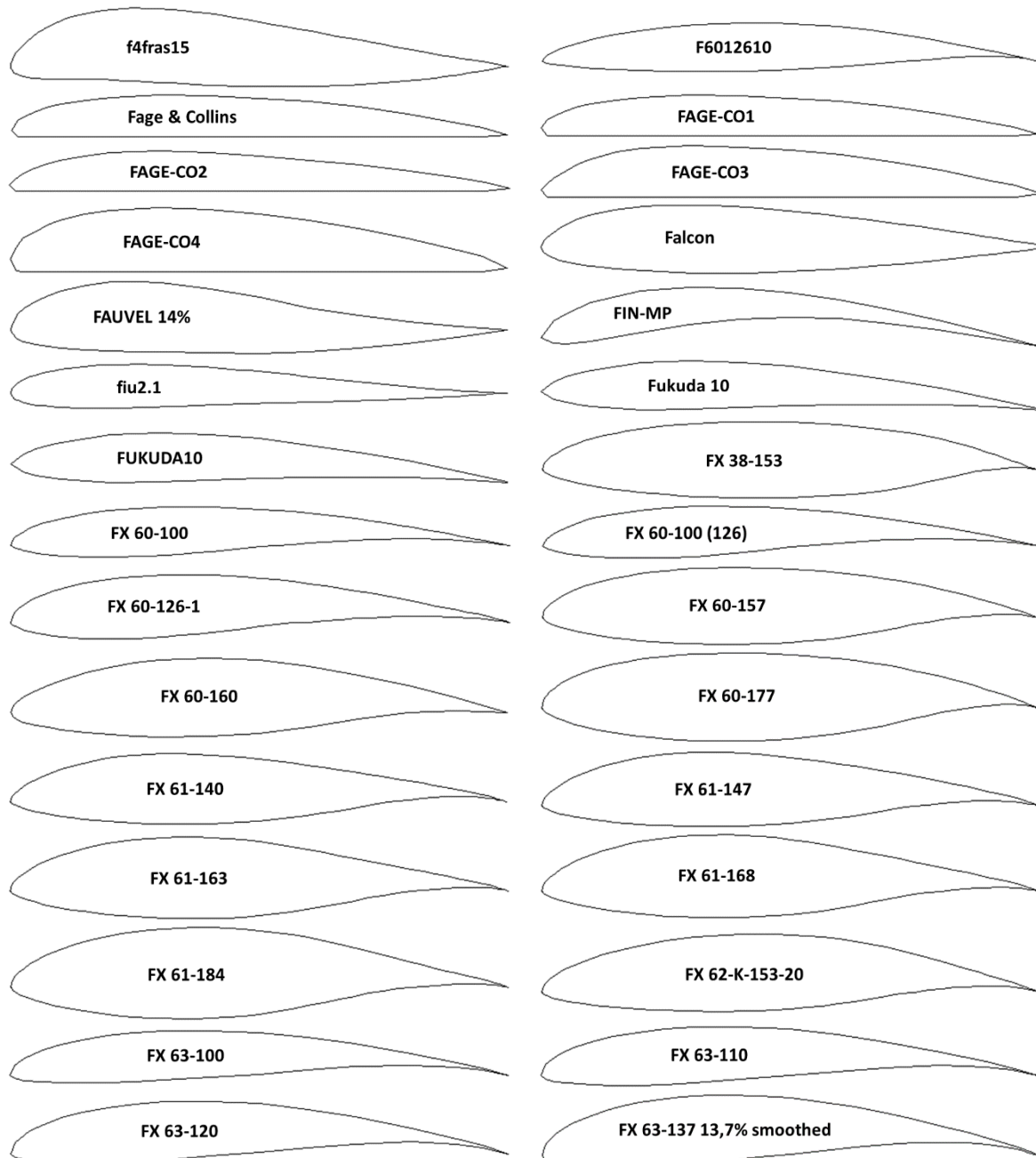
<b>Impact Factor:</b>	<b>ISRA (India) = 6.317</b>	<b>SIS (USA) = 0.912</b>	<b>ICV (Poland) = 6.630</b>
	<b>ISI (Dubai, UAE) = 1.582</b>	<b>РИНЦ (Russia) = 3.939</b>	<b>PIF (India) = 1.940</b>
	<b>GIF (Australia) = 0.564</b>	<b>ESJI (KZ) = 9.035</b>	<b>IBI (India) = 4.260</b>
	<b>JIF = 1.500</b>	<b>SJIF (Morocco) = 7.184</b>	<b>OAJI (USA) = 0.350</b>

<i>FX S 03-182</i>	18.21% at 40.2% of the chord	2.85% at 56.5% of the chord	0.8696%	0.0%
<i>FX05H126</i>	12.61% at 37.1% of the chord	4.4% at 37.1% of the chord	0.8007%	0.0%
<i>FX60-100 10,0% smoothed</i>	9.98% at 27.9% of the chord	3.55% at 56.5% of the chord	0.6674%	0.0%
<i>FX60-126</i>	12.59% at 27.9% of the chord	3.56% at 56.5% of the chord	1.0934%	0.0%
<i>FX62K131</i>	13.09% at 40.2% of the chord	3.89% at 53.3% of the chord	0.5774%	0.0%
<i>FX74_CL5_140</i>	14.05% at 30.9% of the chord	9.94% at 37.1% of the chord	1.4815%	0.0%
<i>FX74-140</i>	14.05% at 30.9% of the chord	9.94% at 37.1% of the chord	1.4815%	0.0%
<i>FX76MPI2</i>	12.07% at 30.0% of the chord	7.61% at 50.0% of the chord	1.2173%	0.175%
<i>FX76MP14</i>	14.04% at 30.0% of the chord	7.09% at 50.0% of the chord	1.6174%	0.182%
<i>FX76MP16</i>	16.09% at 30.0% of the chord	6.06% at 50.0% of the chord	2.1496%	0.018%

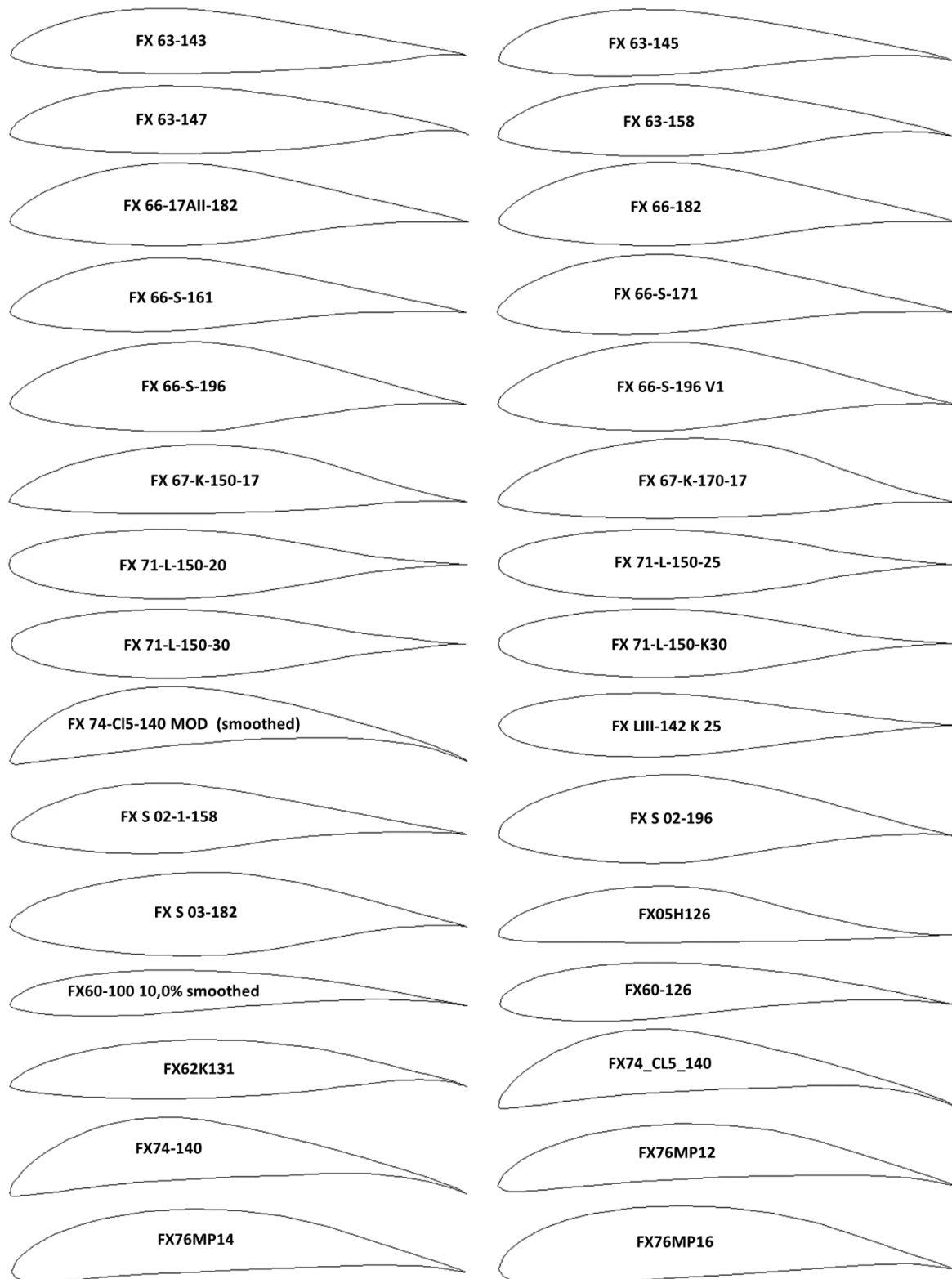
**Note:**

*Fage & Collins* (Great Britain);  
*fiu2.1* (By Matteo Gallizia – Italy);  
*Fukuda 10* (J. Fukuda (Japan)).

**Table 2. The geometric shapes of the airfoils in the cross section.**



<b>Impact Factor:</b>	<b>ISRA (India) = 6.317</b>	<b>SIS (USA) = 0.912</b>	<b>ICV (Poland) = 6.630</b>
	<b>ISI (Dubai, UAE) = 1.582</b>	<b>РИНЦ (Russia) = 3.939</b>	<b>PIF (India) = 1.940</b>
	<b>GIF (Australia) = 0.564</b>	<b>ESJI (KZ) = 9.035</b>	<b>IBI (India) = 4.260</b>
	<b>JIF = 1.500</b>	<b>SJIF (Morocco) = 7.184</b>	<b>OAJI (USA) = 0.350</b>



### Results and discussion

The calculated pressure contours on the surfaces of the airfoils at the different angles of attack are presented in the Figs. 1-60. The calculated magnitudes on the scale can be represented as the basic magnitudes when comparing the pressure drop under

conditions of changing the angle of attack of the airfoils.

Various versions of the airfoils, including smoothed ones, were investigated. Positive pressure at the leading edge of all considered airfoils under conditions of horizontal flight of the airplane was determined in the range of 6.4-6.7 kPa. Thus, the drag

coefficient at the leading edge does not change much. The greatest drag occurs at the leading edge of the FX74-140 airfoil.

The maximum drag occurs in the area of the leading edge of the F6012610 airfoil at the positive angle of attack. The large negative pressure gradient

is formed due to the small radius of the leading edge of this airfoil. However, at the negative angle of attack, negative pressure is reduced by more than 15 times. This calculated magnitude of negative pressure is one of the minimum magnitudes of pressures in conditions of the airplane descent.

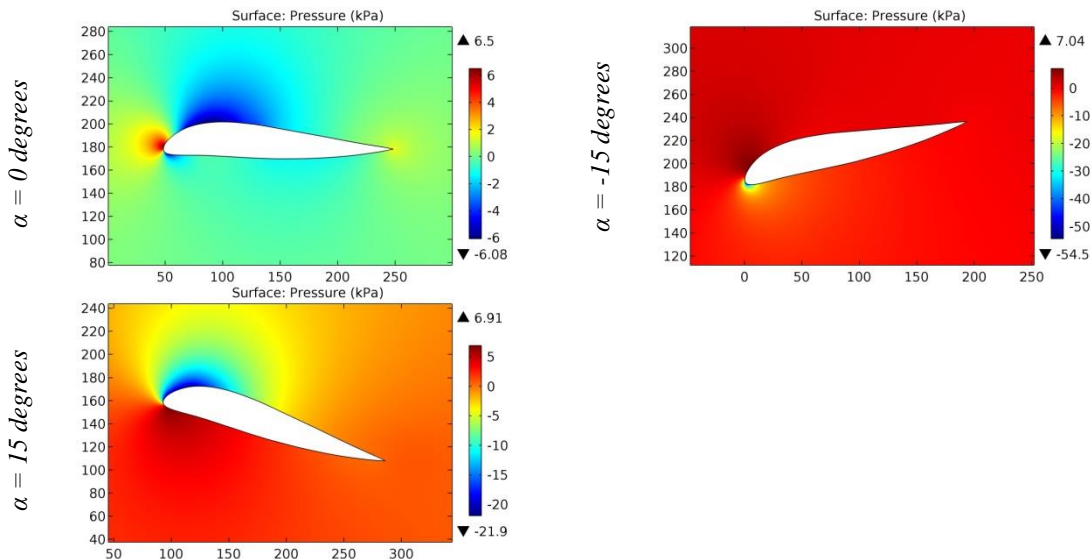


**Figure 1. The pressure contours on the surfaces of the f4fras15 airfoil.**

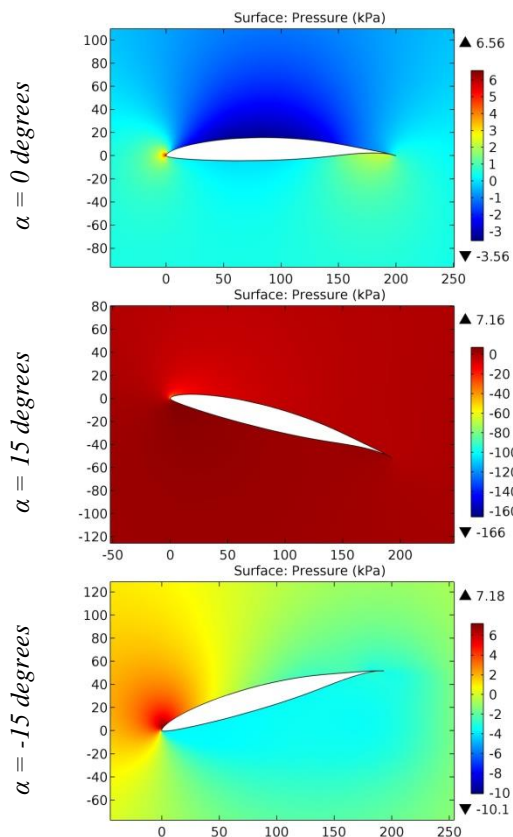


**Figure 2. The pressure contours on the surfaces of the F6012610 airfoil.**

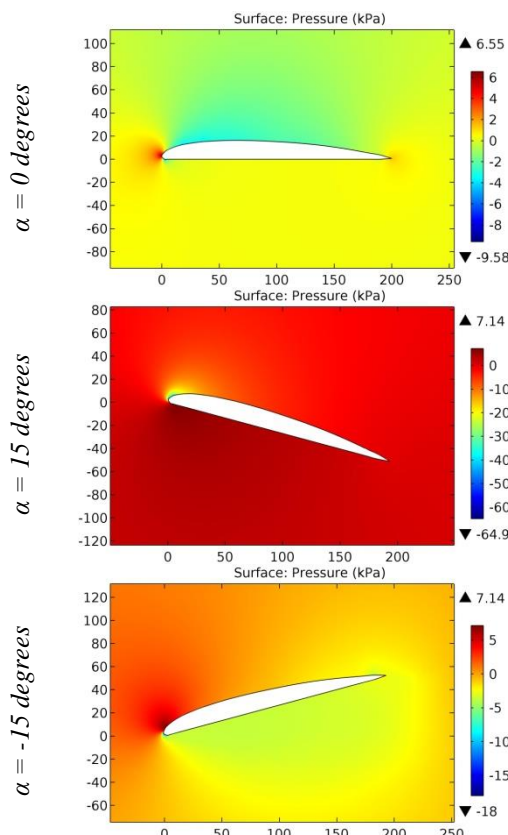


**Figure 3.** The pressure contours on the surfaces of the Fage & Collins airfoil.

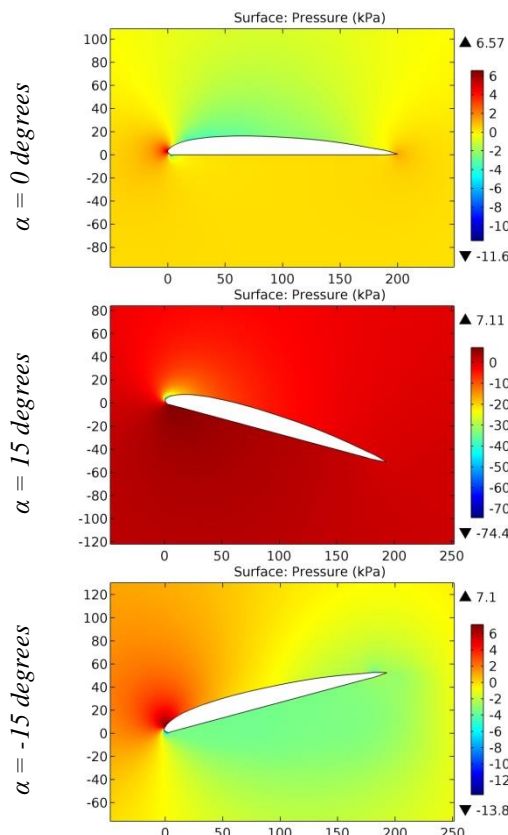


**Figure 4.** The pressure contours on the surfaces of the FAGE-CO1 airfoil.

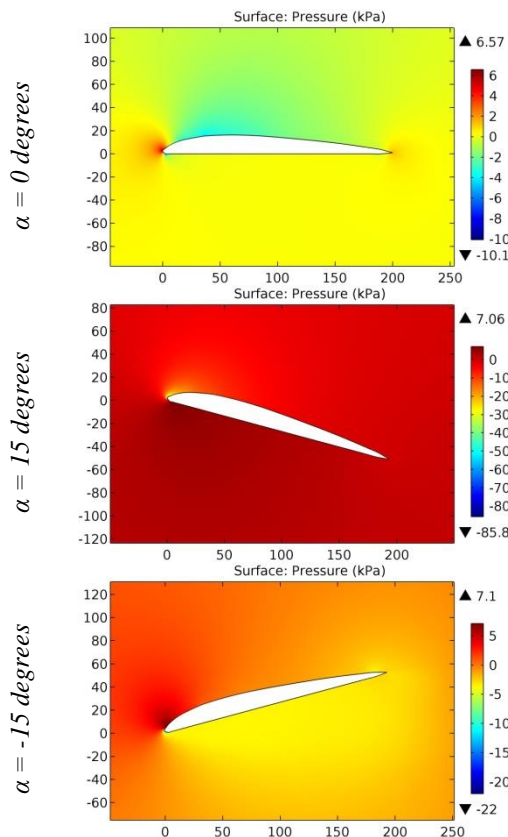


**Figure 5.** The pressure contours on the surfaces of the FAGE-CO2 airfoil.

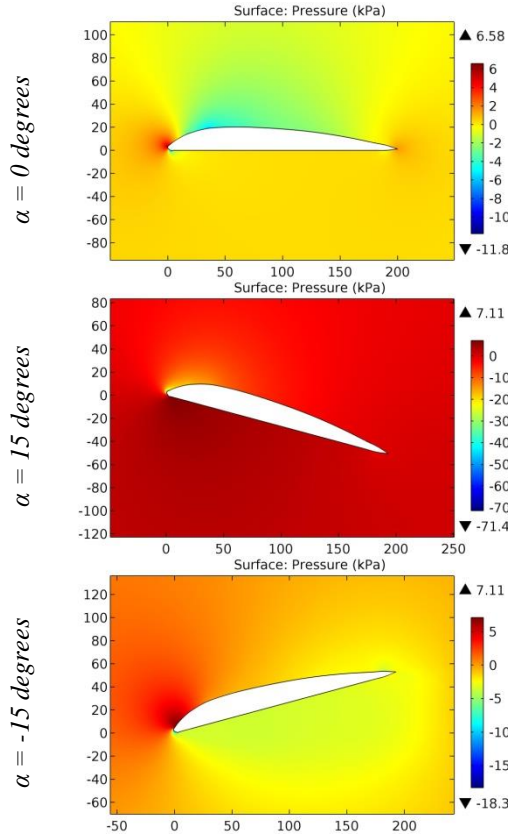


**Figure 6.** The pressure contours on the surfaces of the FAGE-CO3 airfoil.

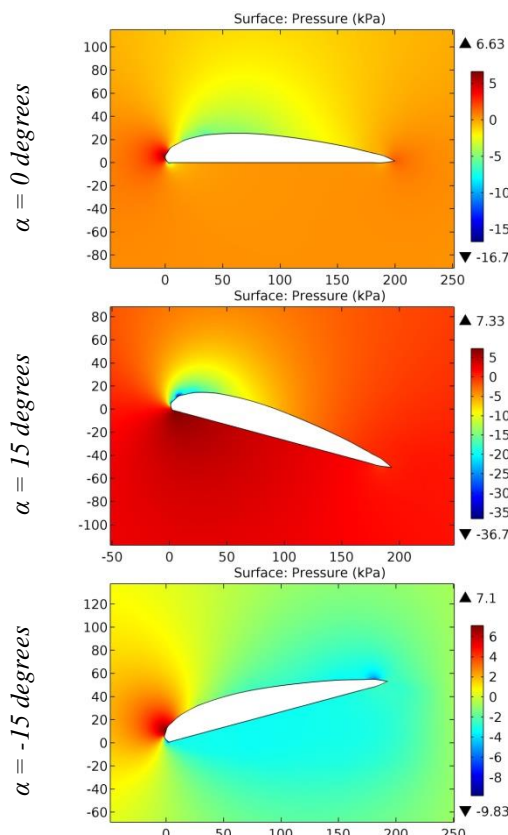


**Figure 7.** The pressure contours on the surfaces of the FAGE-CO4 airfoil.

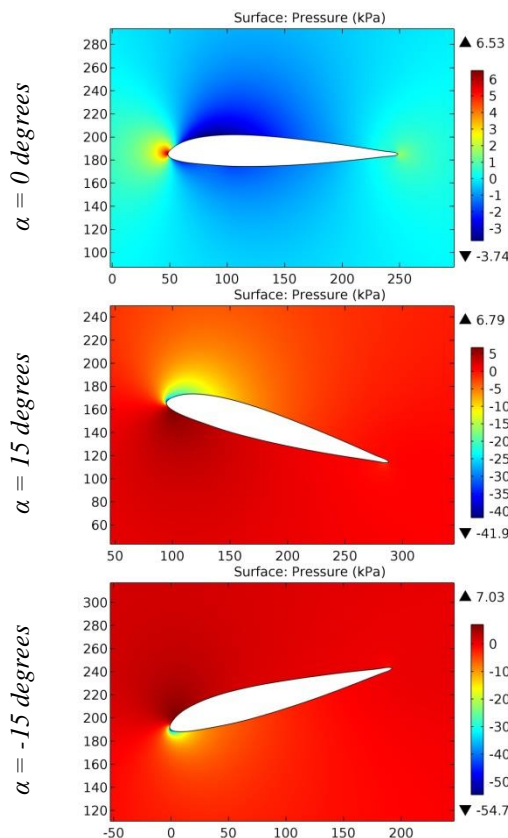


**Figure 8.** The pressure contours on the surfaces of the Falcon airfoil.

ISRA (India)	= 6.317	SIS (USA)	= 0.912	ICV (Poland)	= 6.630
ISI (Dubai, UAE)	= 1.582	РИНЦ (Russia)	= 3.939	PIF (India)	= 1.940
GIF (Australia)	= 0.564	ESJI (KZ)	= 9.035	IBI (India)	= 4.260
JIF	= 1.500	SJIF (Morocco)	= 7.184	OAJI (USA)	= 0.350

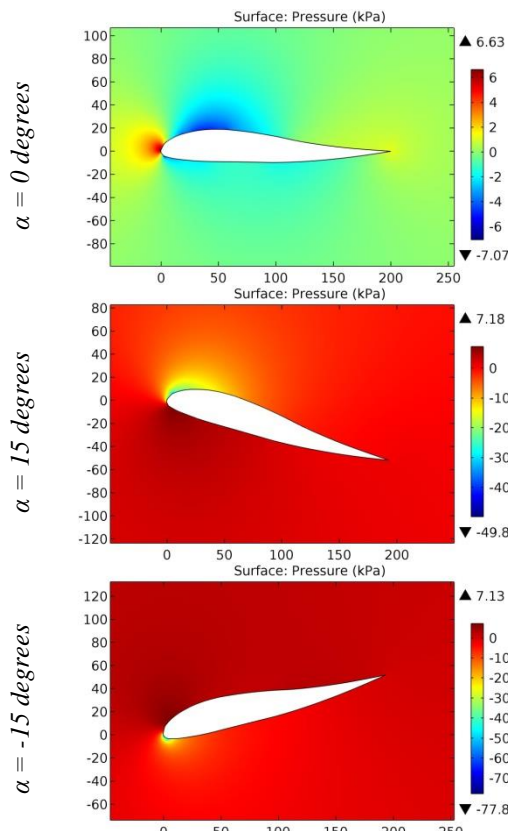


**Figure 9.** The pressure contours on the surfaces of the FAUVEL 14% airfoil.

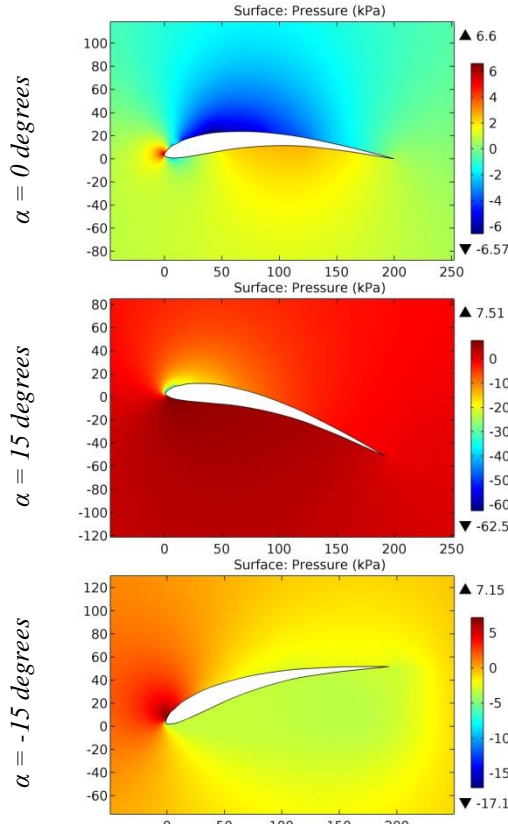


**Figure 10.** The pressure contours on the surfaces of the FIN-MP airfoil.

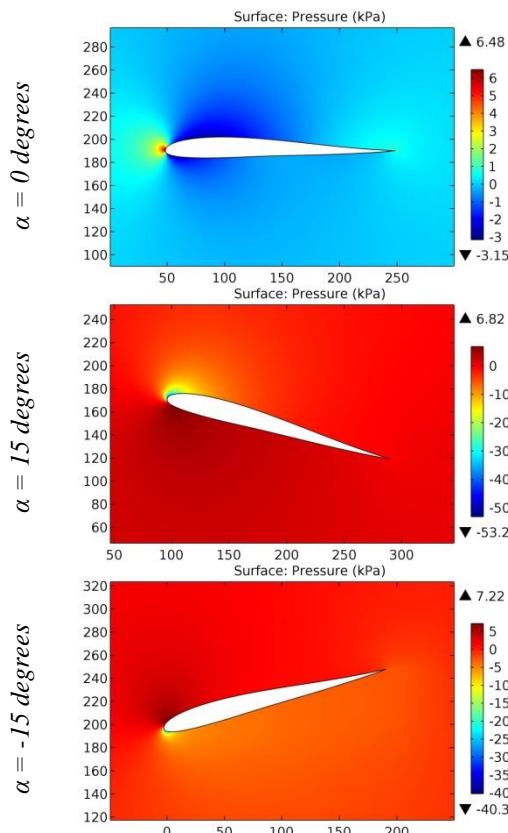


**Figure 11.** The pressure contours on the surfaces of the fiu2.1 airfoil.

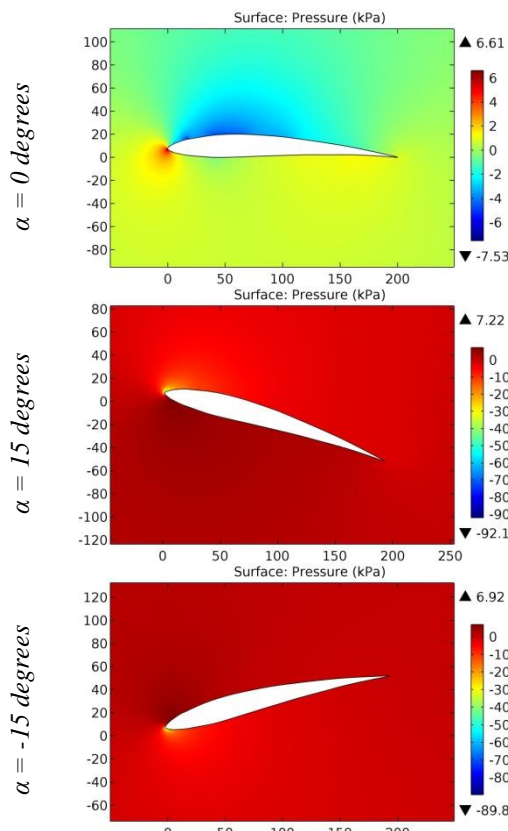


**Figure 12.** The pressure contours on the surfaces of the Fukuda 10 airfoil.

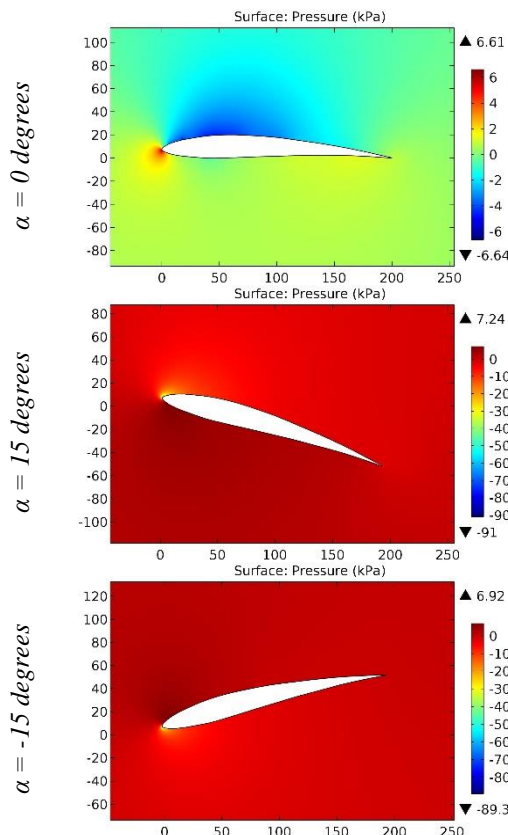


**Figure 13.** The pressure contours on the surfaces of the FUKUDA10 airfoil.

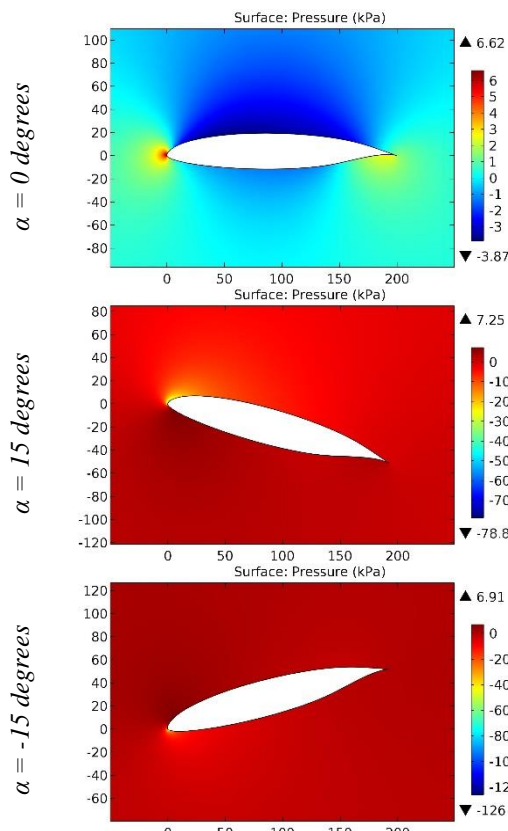


**Figure 14.** The pressure contours on the surfaces of the FX 38-153 airfoil.

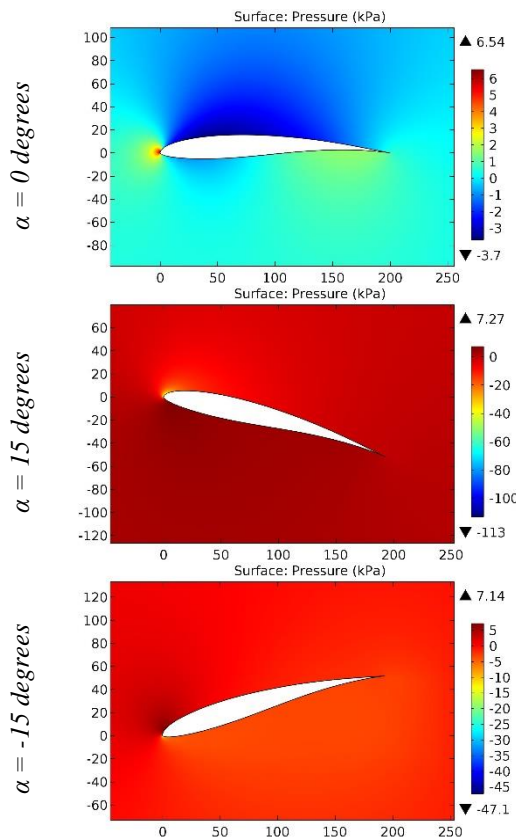


**Figure 15.** The pressure contours on the surfaces of the FX 60-100 airfoil.

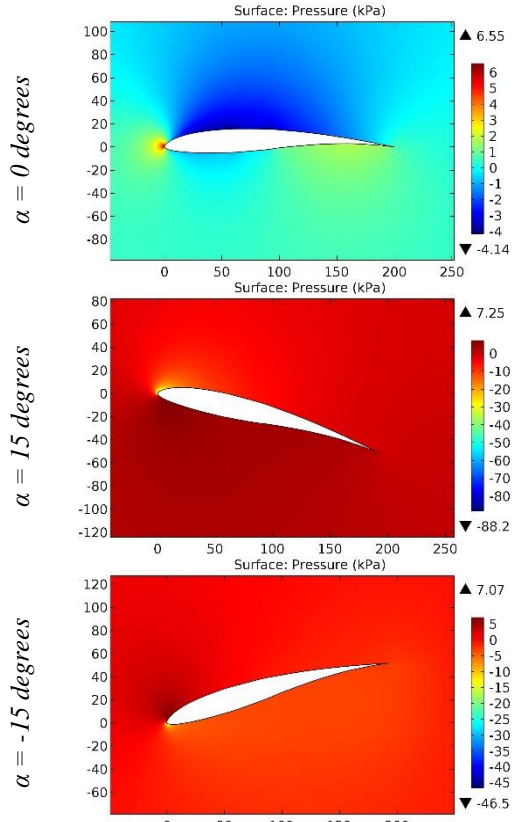


**Figure 16.** The pressure contours on the surfaces of the FX 60-100 (126) airfoil.

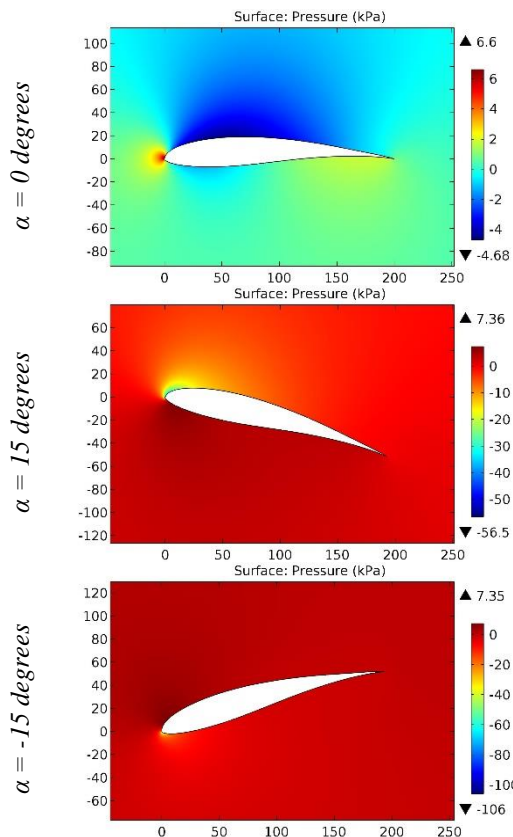


**Figure 17.** The pressure contours on the surfaces of the FX 60-126-1 airfoil.

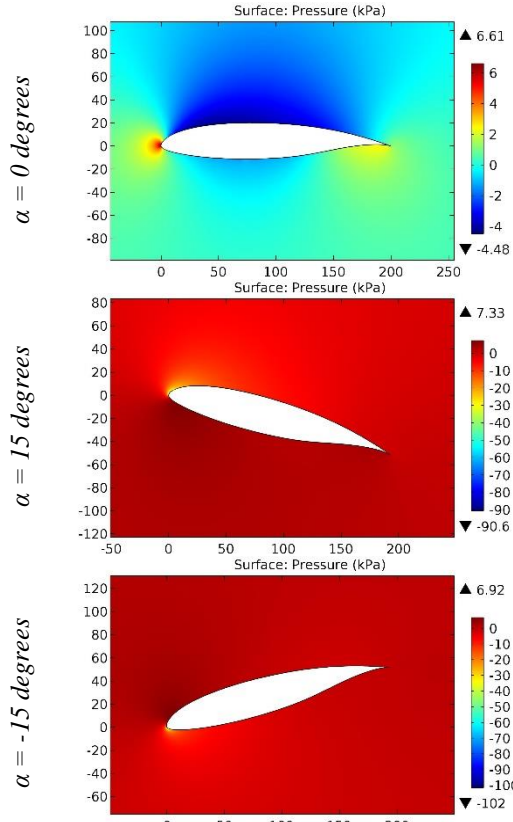


**Figure 18.** The pressure contours on the surfaces of the FX 60-157 airfoil.

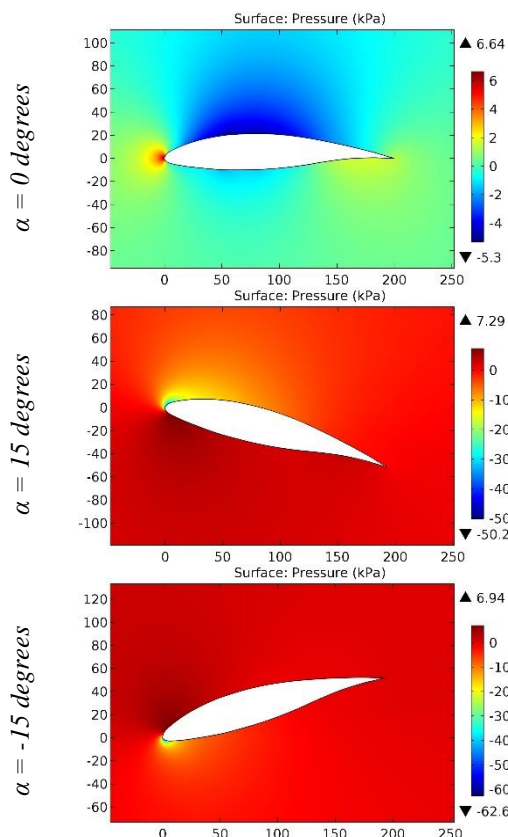


**Figure 19.** The pressure contours on the surfaces of the FX 60-160 airfoil.

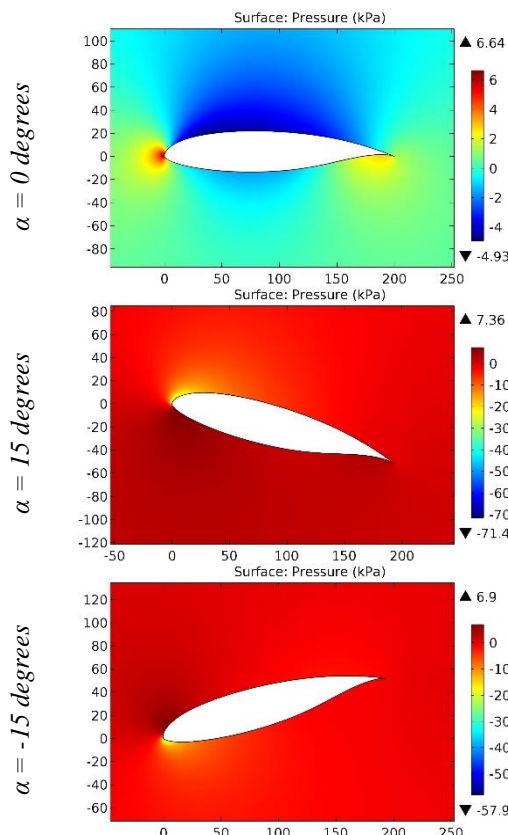


**Figure 20.** The pressure contours on the surfaces of the FX 60-177 airfoil.

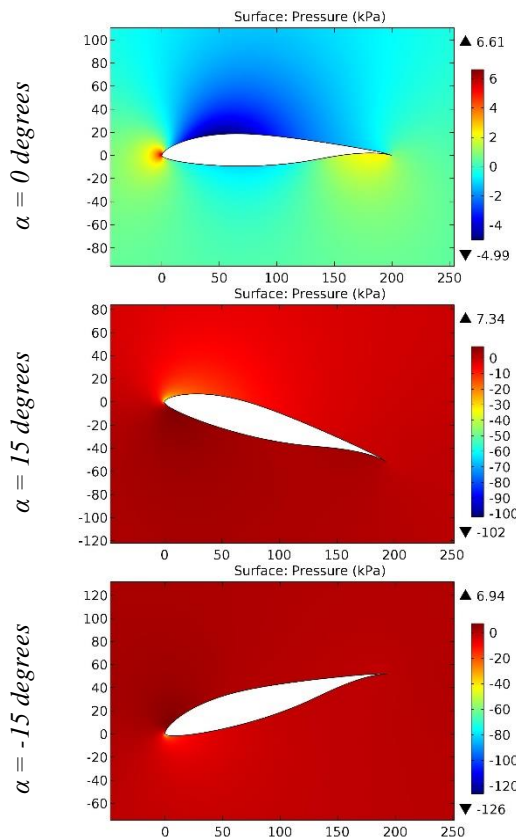


**Figure 21.** The pressure contours on the surfaces of the FX 61-140 airfoil.

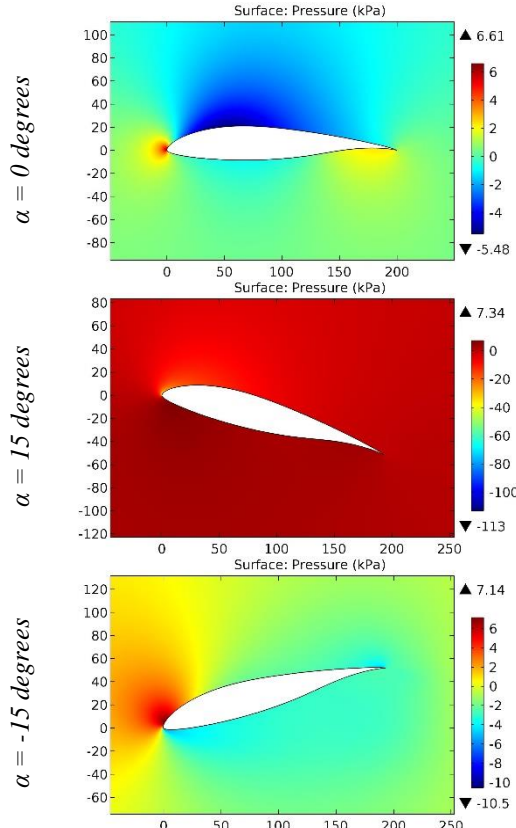


**Figure 22.** The pressure contours on the surfaces of the FX 61-147 airfoil.

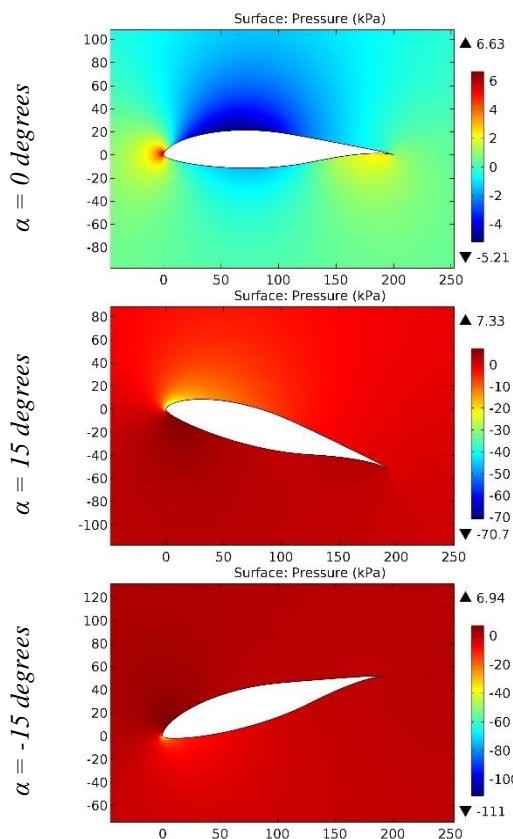


**Figure 23.** The pressure contours on the surfaces of the FX 61-163 airfoil.

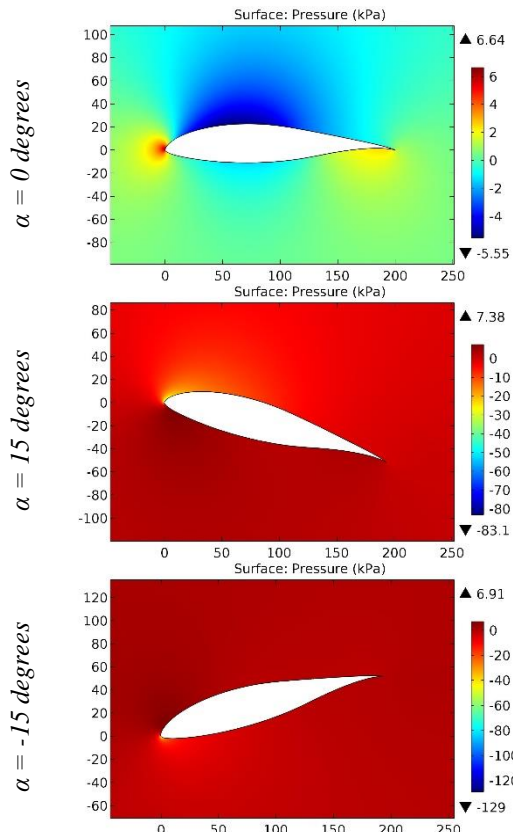


**Figure 24.** The pressure contours on the surfaces of the FX 61-168 airfoil.

ISRA (India)	= 6.317	SIS (USA)	= 0.912	ICV (Poland)	= 6.630
ISI (Dubai, UAE)	= 1.582	РИНЦ (Russia)	= 3.939	PIF (India)	= 1.940
GIF (Australia)	= 0.564	ESJI (KZ)	= 9.035	IBI (India)	= 4.260
JIF	= 1.500	SJIF (Morocco)	= 7.184	OAJI (USA)	= 0.350

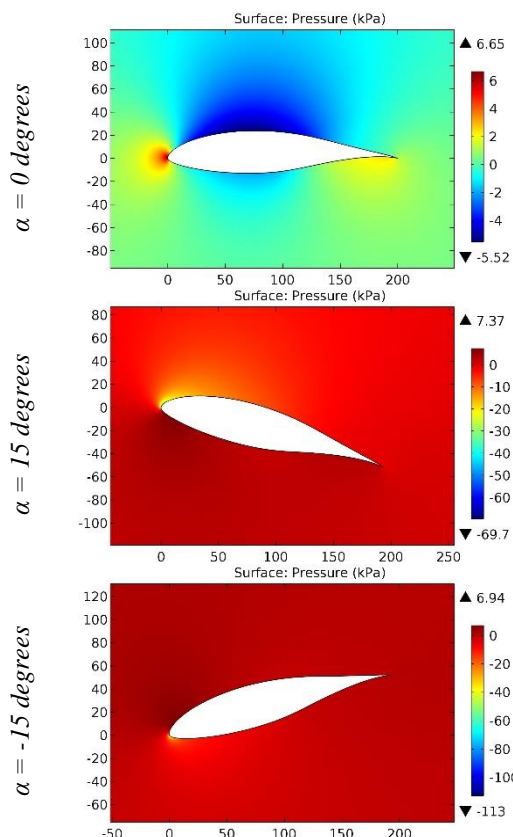


**Figure 25.** The pressure contours on the surfaces of the FX 61-184 airfoil.

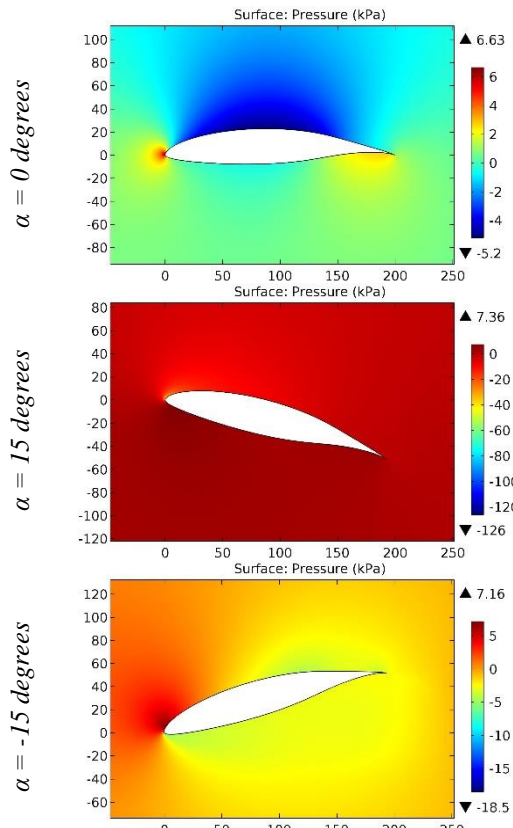


**Figure 26.** The pressure contours on the surfaces of the FX 62-K-153-20 airfoil.

ISRA (India) = 6.317	SIS (USA) = 0.912	ICV (Poland) = 6.630
ISI (Dubai, UAE) = 1.582	РИНЦ (Russia) = 3.939	PIF (India) = 1.940
GIF (Australia) = 0.564	ESJI (KZ) = 9.035	IBI (India) = 4.260
JIF = 1.500	SJIF (Morocco) = 7.184	OAJI (USA) = 0.350

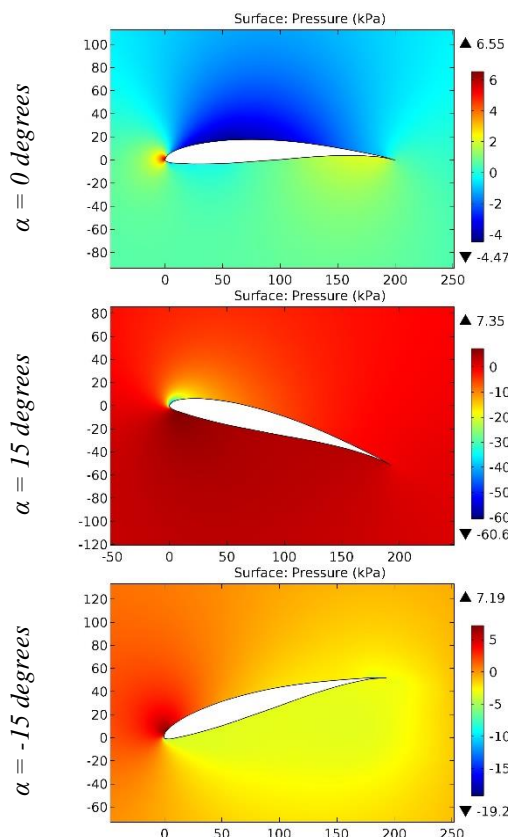


Figure 27. The pressure contours on the surfaces of the FX 63-100 airfoil.

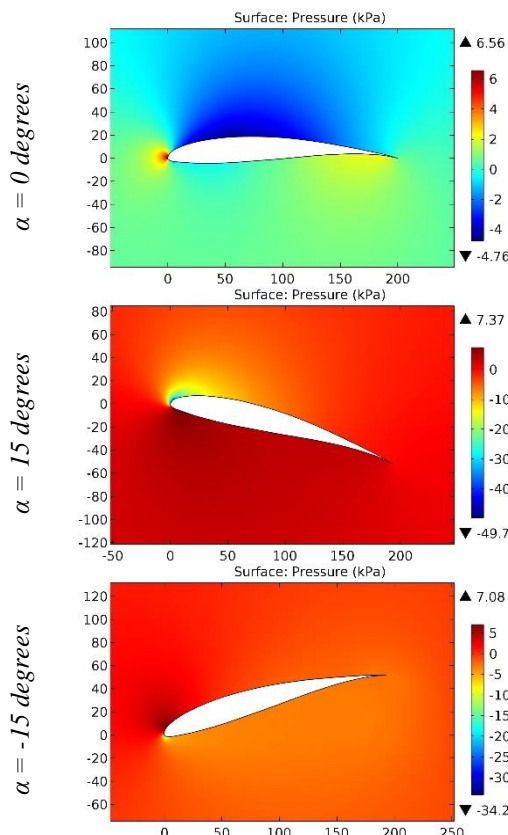
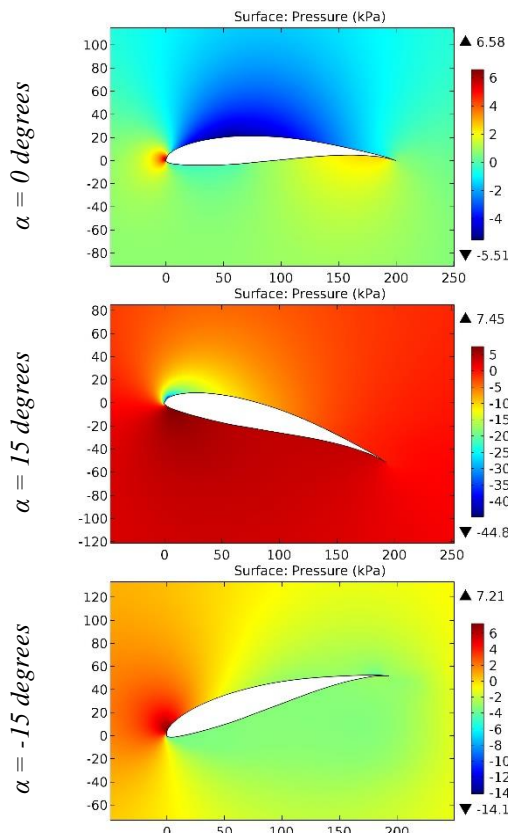
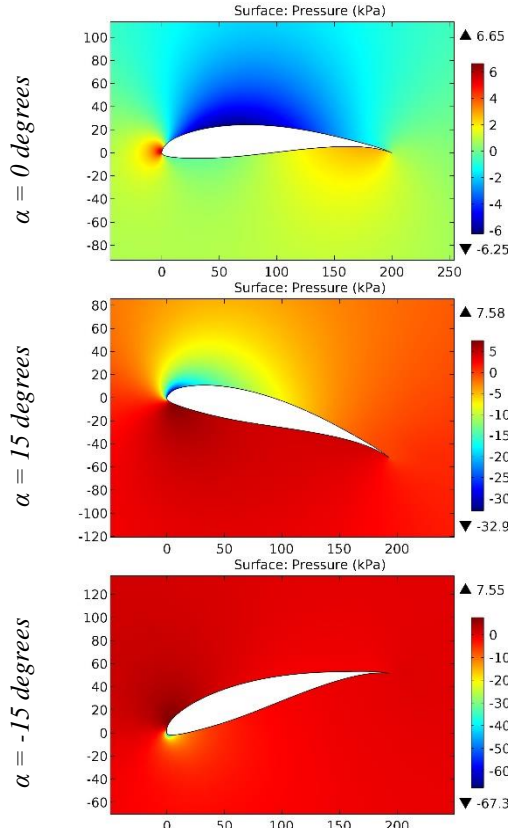


Figure 28. The pressure contours on the surfaces of the FX 63-110 airfoil.



**Figure 29.** The pressure contours on the surfaces of the FX 63-120 airfoil.



**Figure 30.** The pressure contours on the surfaces of the FX 63-137 13,7% (smoothed) airfoil.

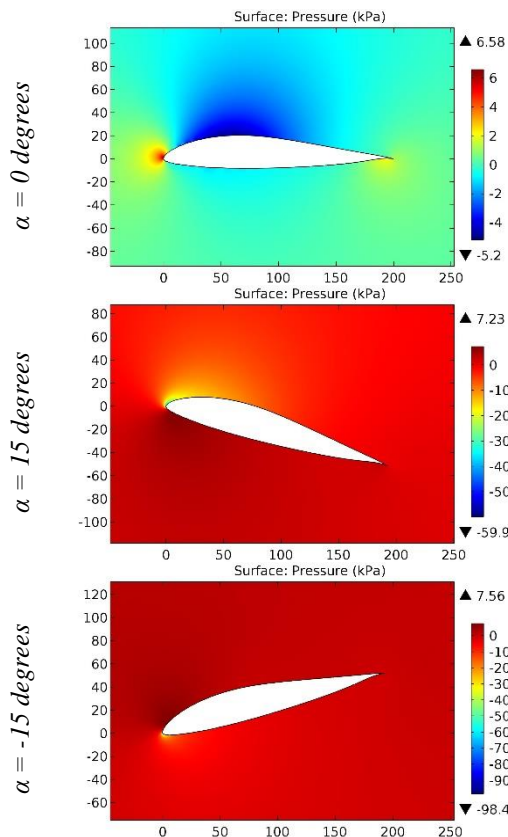


**Figure 31.** The pressure contours on the surfaces of the FX 63-143 airfoil.

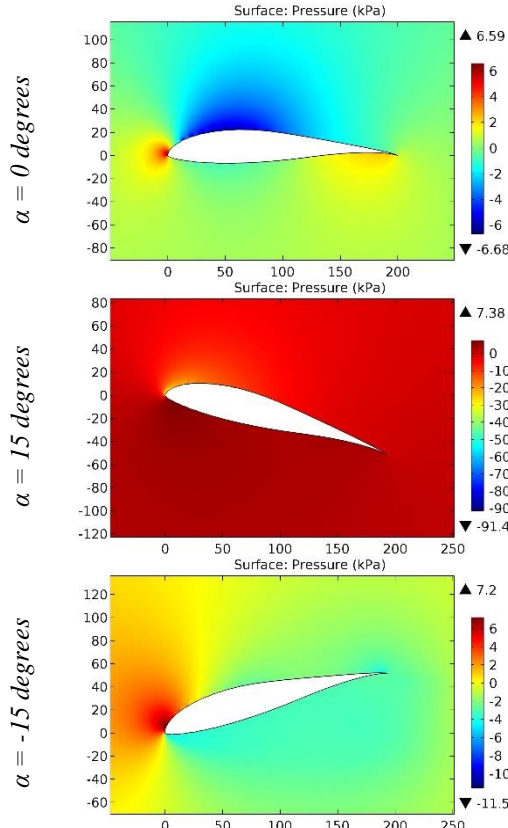


**Figure 32.** The pressure contours on the surfaces of the FX 63-145 airfoil.

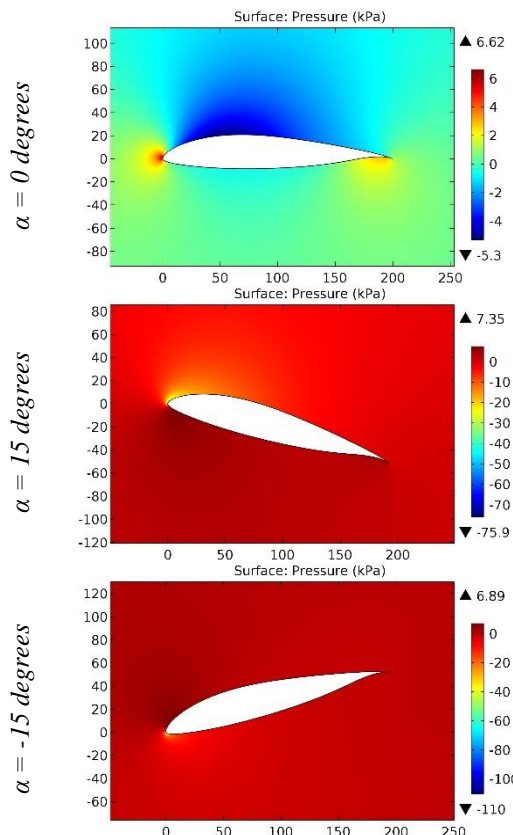


**Figure 33.** The pressure contours on the surfaces of the FX 63-147 airfoil.

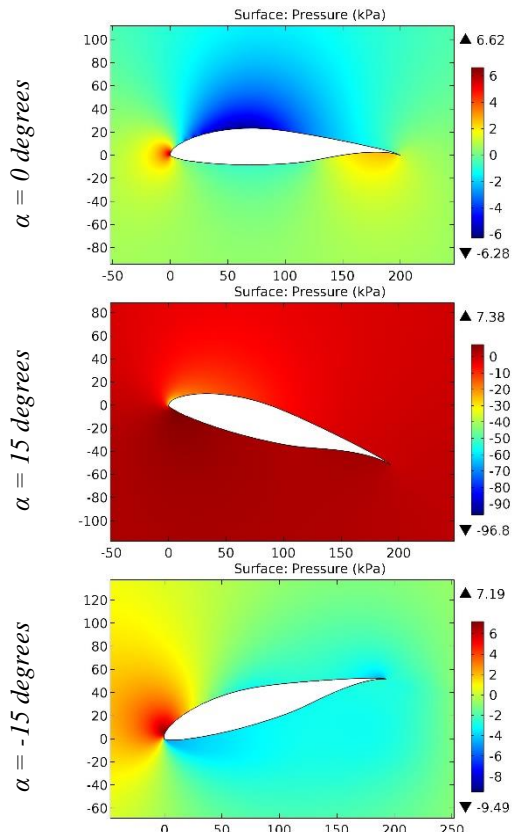


**Figure 34.** The pressure contours on the surfaces of the FX 63-158 airfoil.

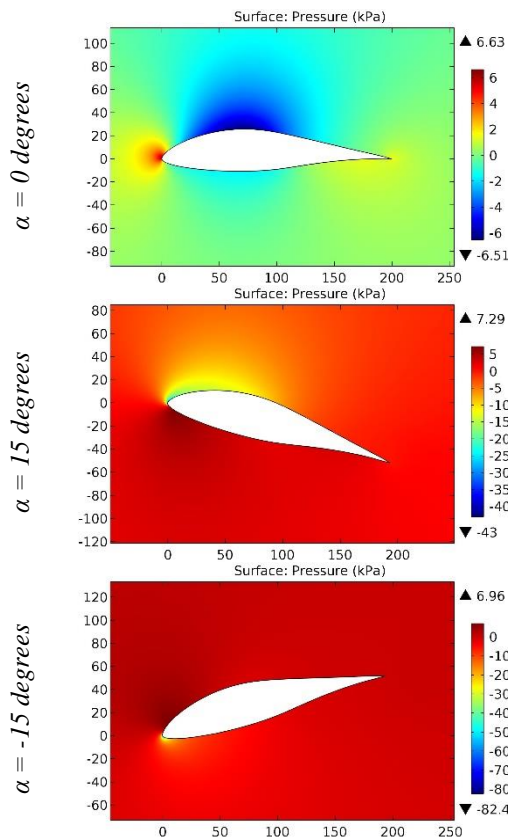


**Figure 35.** The pressure contours on the surfaces of the FX 66-17AII-182 airfoil.

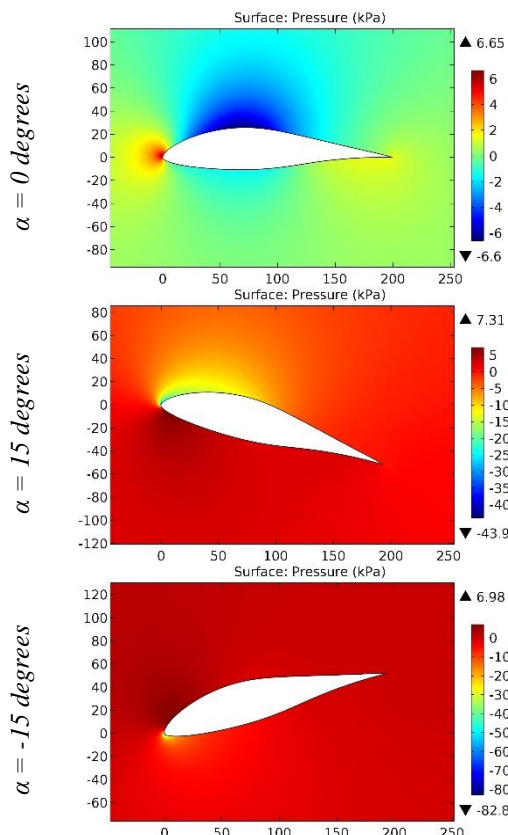


**Figure 36.** The pressure contours on the surfaces of the FX 66-182 airfoil.

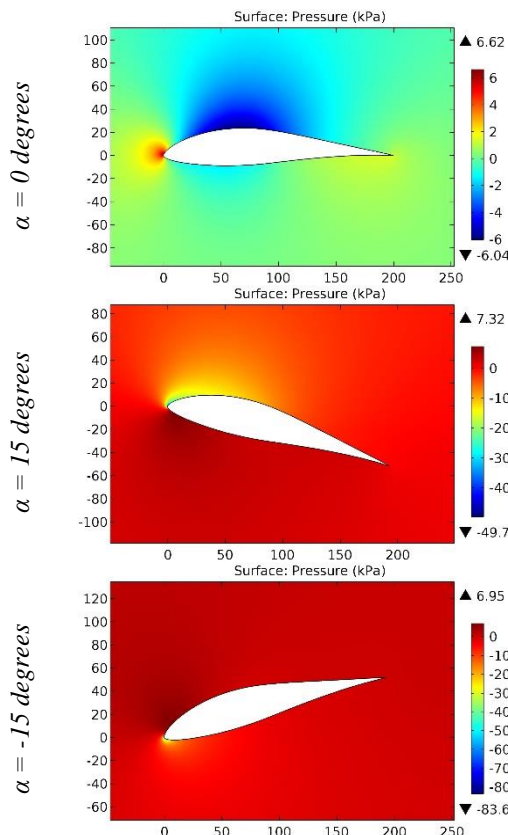


**Figure 37.** The pressure contours on the surfaces of the FX 66-S-161 airfoil.

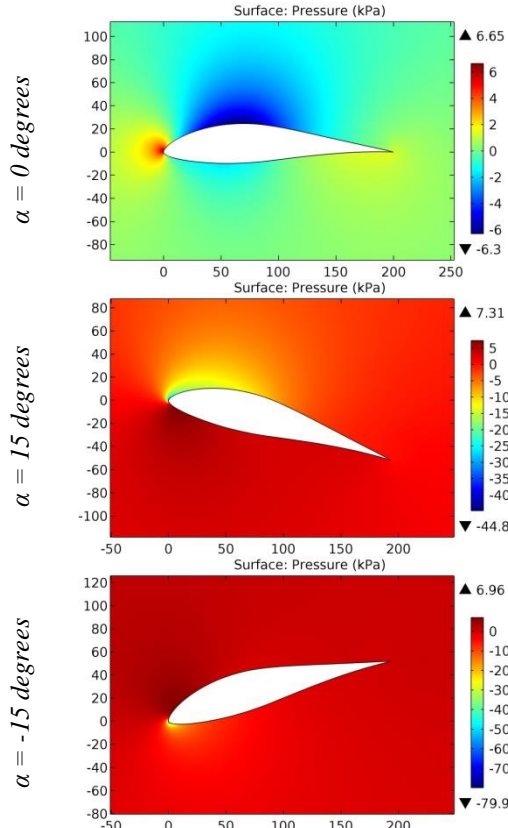


**Figure 38.** The pressure contours on the surfaces of the FX 66-S-171 airfoil.

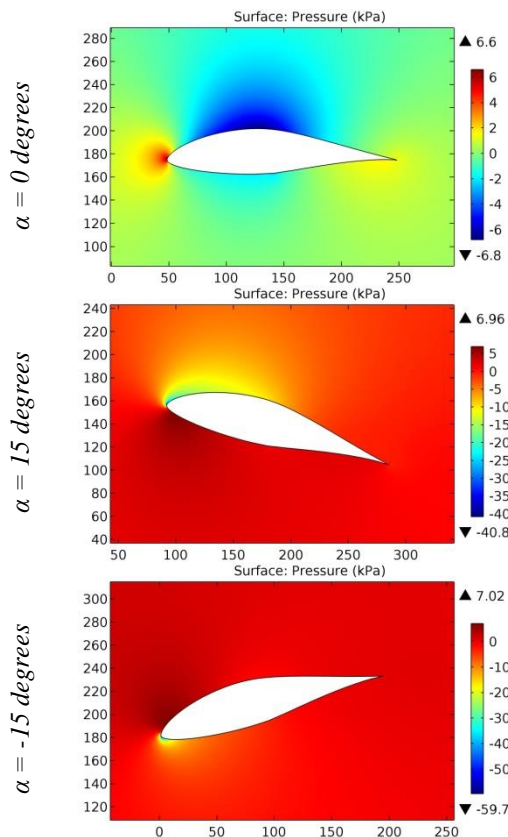


**Figure 39.** The pressure contours on the surfaces of the FX 66-S-196 airfoil.

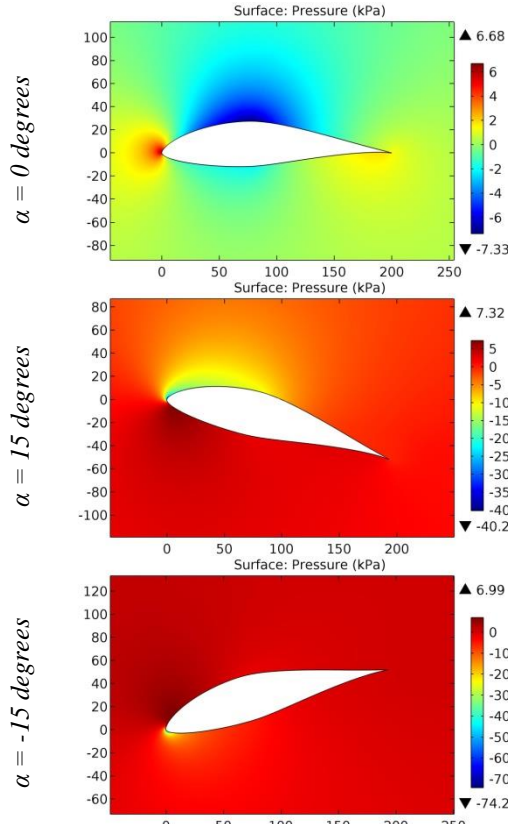


**Figure 40.** The pressure contours on the surfaces of the FX 66-S-196 V1 airfoil.

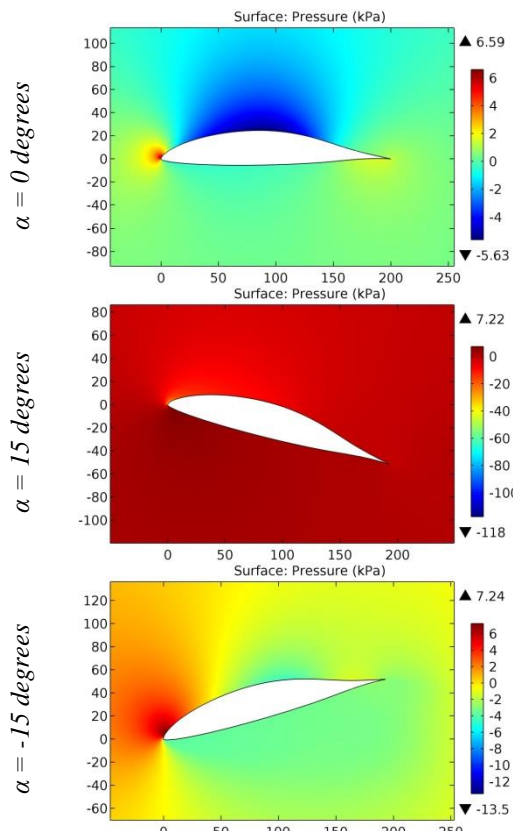


**Figure 41.** The pressure contours on the surfaces of the FX 67-K-150-17 airfoil.

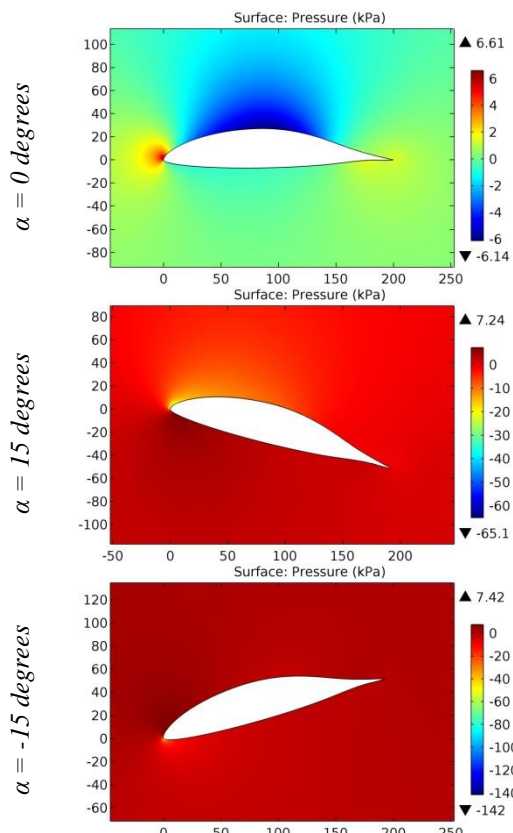


**Figure 42.** The pressure contours on the surfaces of the FX 67-K-170-17 airfoil.

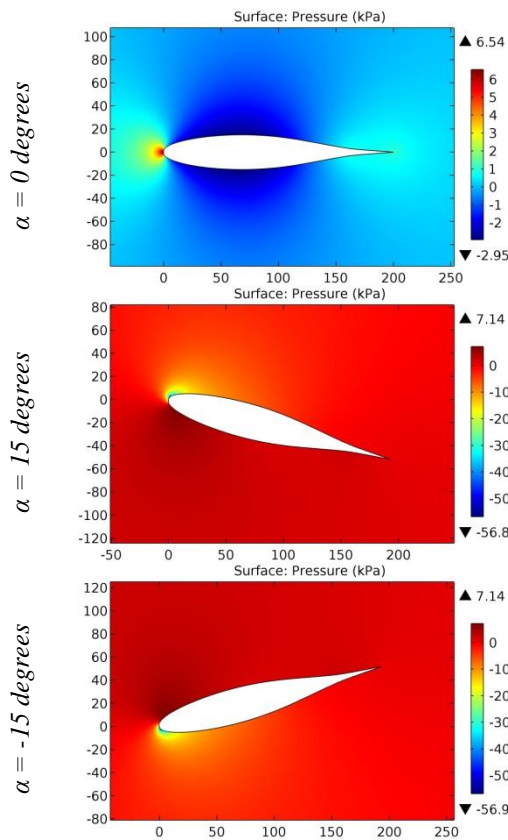


**Figure 43.** The pressure contours on the surfaces of the FX 71-L-150-20 airfoil.

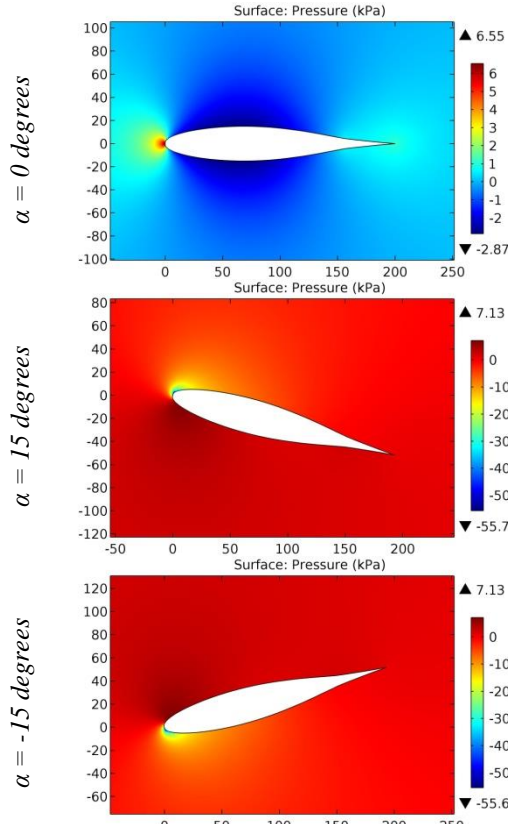


**Figure 44.** The pressure contours on the surfaces of the FX 71-L-150-25 airfoil.

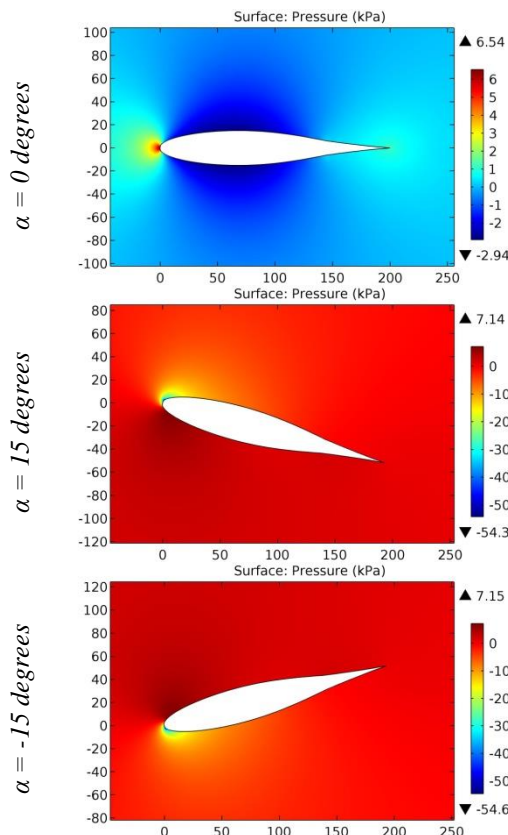


**Figure 45.** The pressure contours on the surfaces of the FX 71-L-150-30 airfoil.

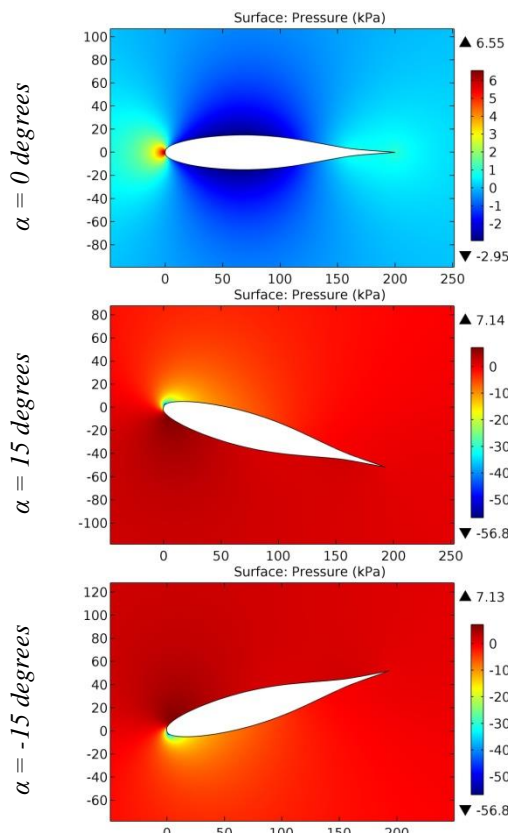


**Figure 46.** The pressure contours on the surfaces of the FX 71-L-150-K30 airfoil.

ISRA (India) = 6.317	SIS (USA) = 0.912	ICV (Poland) = 6.630
ISI (Dubai, UAE) = 1.582	РИНЦ (Russia) = 3.939	PIF (India) = 1.940
GIF (Australia) = 0.564	ESJI (KZ) = 9.035	IBI (India) = 4.260
JIF = 1.500	SJIF (Morocco) = 7.184	OAJI (USA) = 0.350

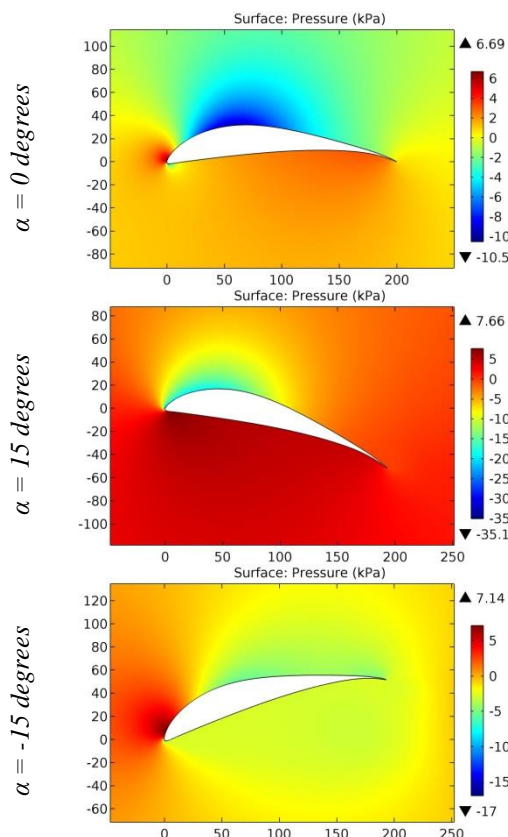


**Figure 47.** The pressure contours on the surfaces of the FX 74-Cl5-140 MOD (smoothed) airfoil.

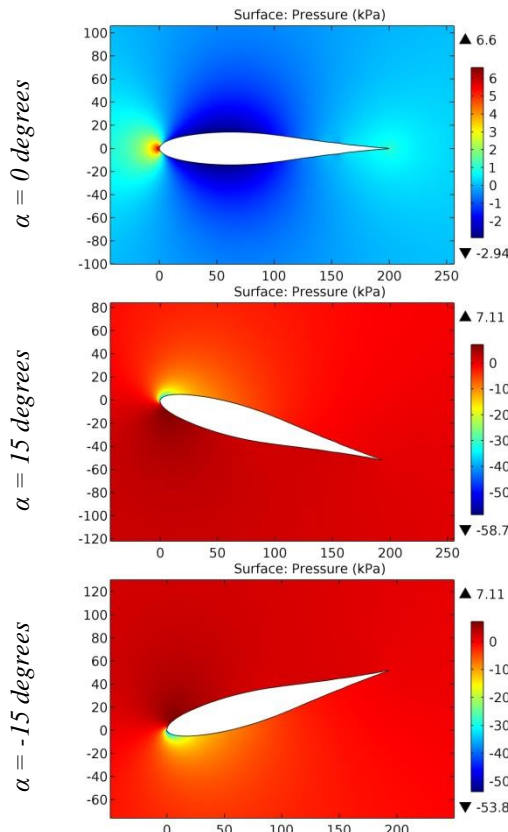


**Figure 48.** The pressure contours on the surfaces of the FX LIII-142 K 25 airfoil.

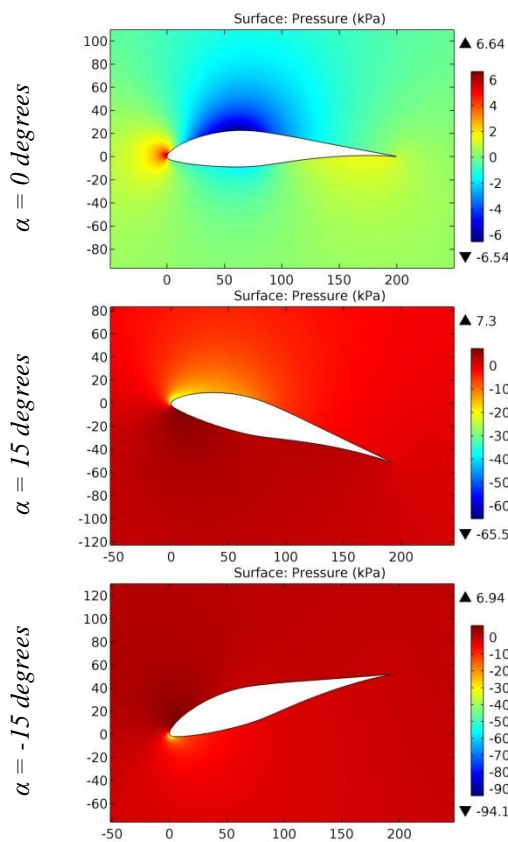


**Figure 49.** The pressure contours on the surfaces of the FX S 02-1-158 airfoil.

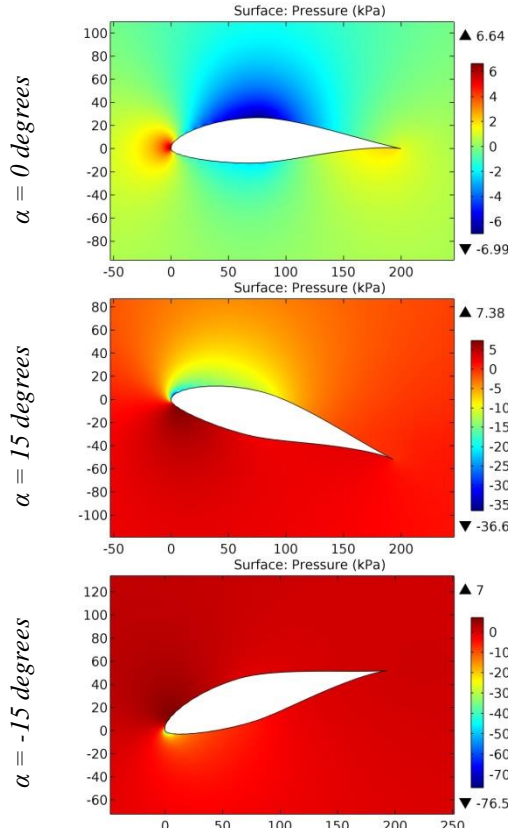


**Figure 50.** The pressure contours on the surfaces of the FX S 02-196 airfoil.

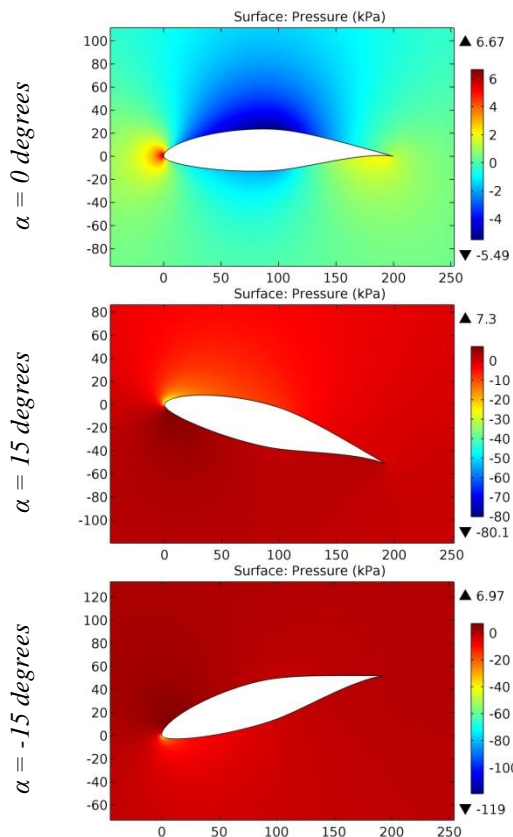


**Figure 51.** The pressure contours on the surfaces of the FX S 03-182 airfoil.

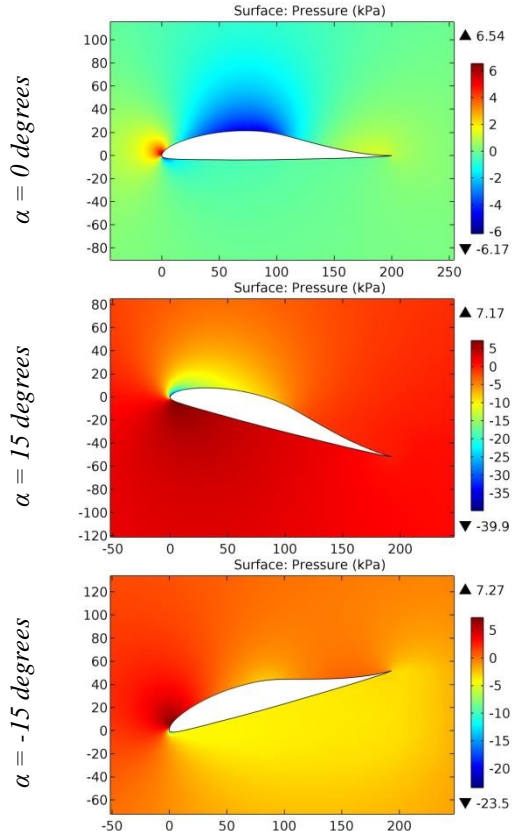


**Figure 52.** The pressure contours on the surfaces of the FX05H126 airfoil.

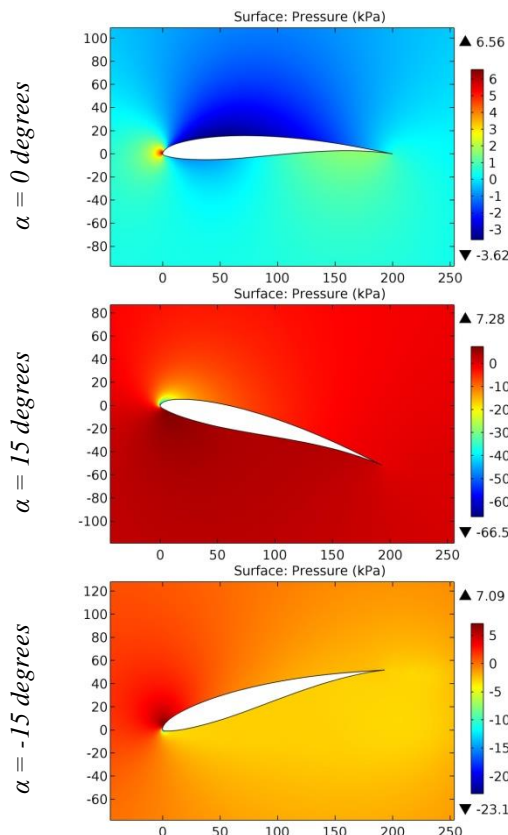


**Figure 53.** The pressure contours on the surfaces of the FX60-100 10,0% smoothed airfoil.

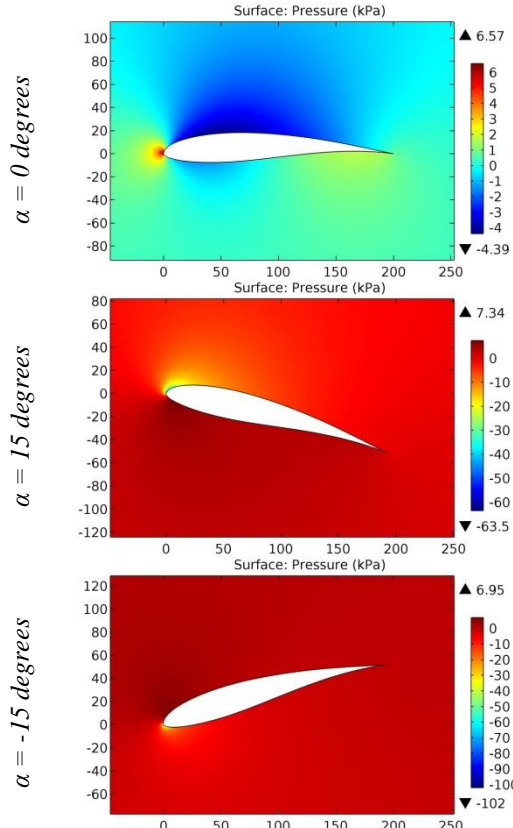


**Figure 54.** The pressure contours on the surfaces of the FX60-126 airfoil.

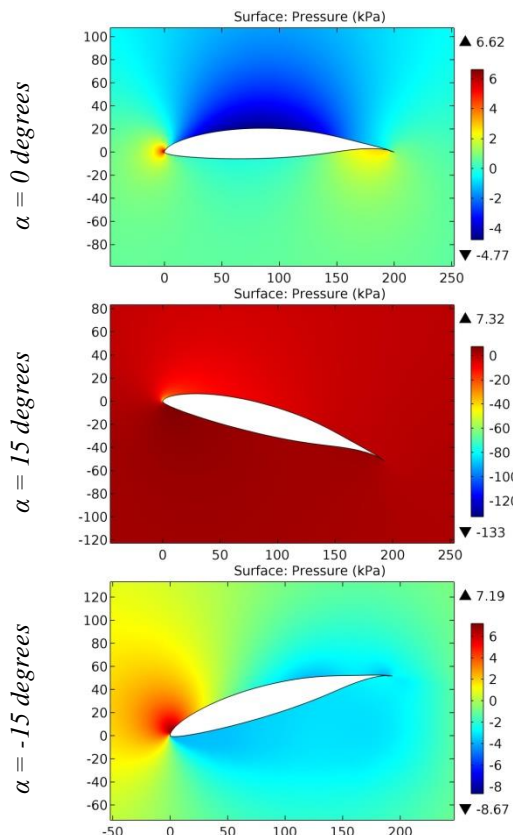


**Figure 55.** The pressure contours on the surfaces of the FX62K131 airfoil.

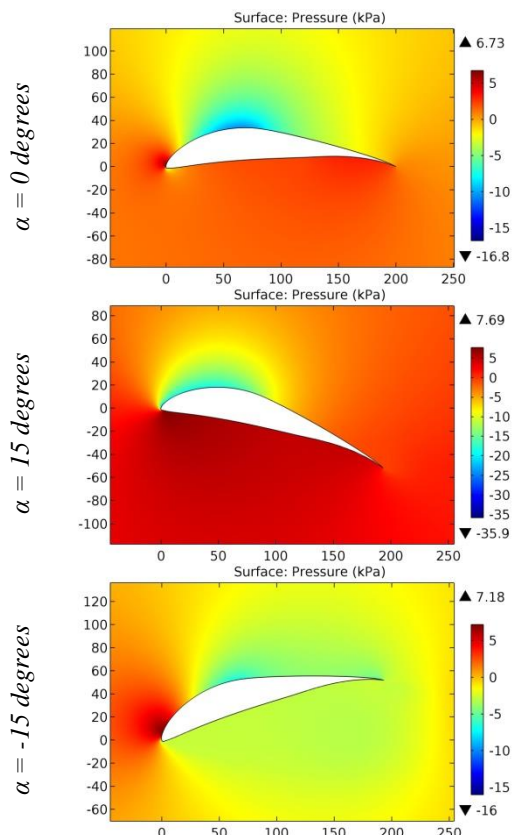


**Figure 56.** The pressure contours on the surfaces of the FX74\_CL5\_140 airfoil.

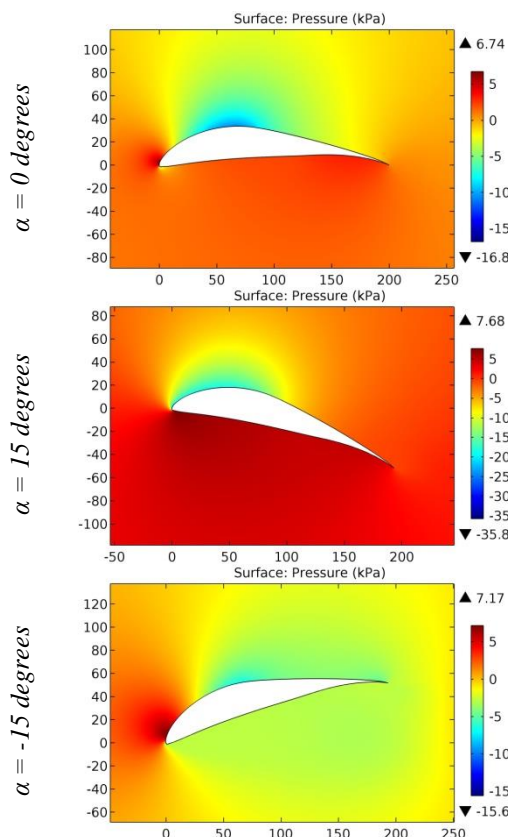


**Figure 57.** The pressure contours on the surfaces of the FX74-140 airfoil.

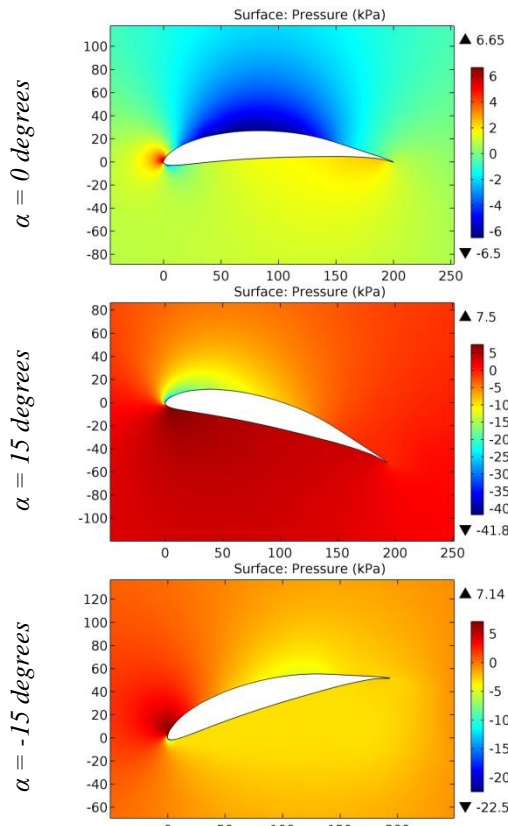


**Figure 58.** The pressure contours on the surfaces of the FX76MP12 airfoil.

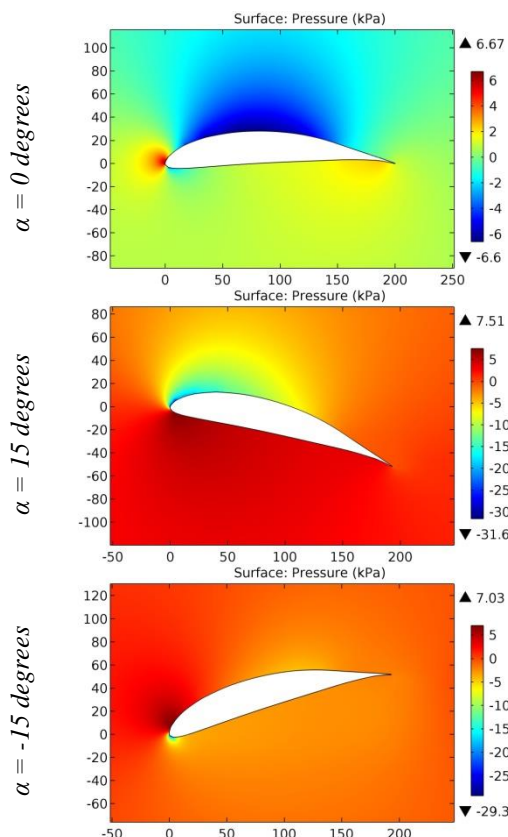


**Figure 59.** The pressure contours on the surfaces of the FX76MP14 airfoil.

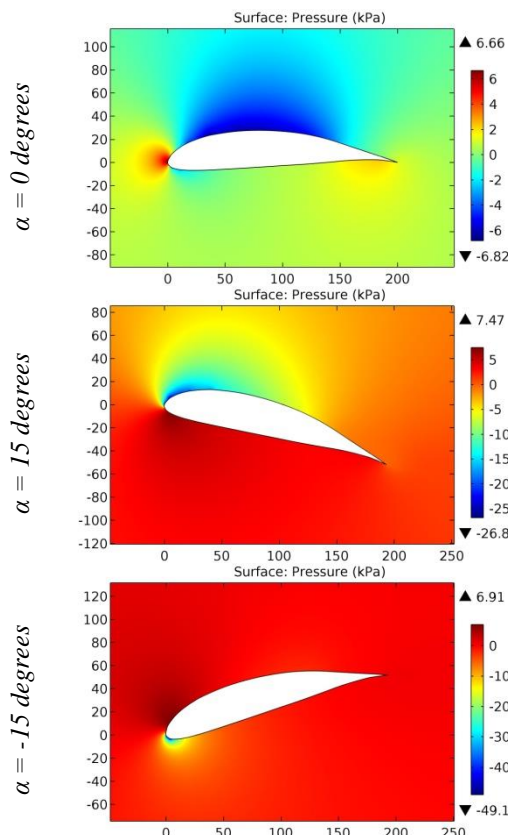


**Figure 60.** The pressure contours on the surfaces of the FX76MP16 airfoil.

## Impact Factor:

ISRA (India) = **6.317**  
ISI (Dubai, UAE) = **1.582**  
GIF (Australia) = **0.564**  
JIF = **1.500**

SIS (USA) = **0.912**  
РИНЦ (Russia) = **3.939**  
ESJI (KZ) = **9.035**  
SJIF (Morocco) = **7.184**

ICV (Poland) = **6.630**  
PIF (India) = **1.940**  
IBI (India) = **4.260**  
OAJI (USA) = **0.350**

The maximum increase in pressure at the leading edge occurs at the angle of attack of 15 degrees for the following airfoils: F6012610, Fage & Collins, FAGE-CO1, FAGE-CO2, FAGE-CO3, FAGE-CO4, FIN-MP, fiu2.1, Fukuda 10, FUKUDA10, FX 60-100, FX 60-100 (126), FX 60-177, FX 61-147, FX 62-K-153-20, FX 63-100, FX 63-110, FX 63-120, FX 63-145, FX 63-158, FX 67-K-150-17, FX 71-L-150-25, FX 74-CI5-140 MOD (smoothed), FX LIII-142 K 25, FX05H126, FX60-100 10,0% smoothed, FX62K131, FX74\_CL5\_140, FX74-140, FX76MP12, FX76MP14. The maximum increase in pressure at the leading edge occurs at the angle of attack of -15 degrees for the remaining airfoils.

## Conclusion

The airfoils without curvature are affected by following pressures during horizontal flight of the airplane: negative (near the upper surface) and positive (near the leading and trailing edges and the lower surface). The thin (medium thickness) airfoils with the small leading edge radius create the high drag when the airplane climb and the low drag when the airplane descent. Negative pressure increases at the negative angle of attack and decreases at the positive angle of attack with an increase in the leading edge radius of the airfoil with a thickening in the middle (for example, FX60-126).

## References:

1. Anderson, J. D. (2010). *Fundamentals of Aerodynamics*. McGraw-Hill, Fifth edition.
2. Shevell, R. S. (1989). *Fundamentals of Flight*. Prentice Hall, Second edition.
3. Houghton, E. L., & Carpenter, P. W. (2003). *Aerodynamics for Engineering Students*. Fifth edition, Elsevier.
4. Lan, E. C. T., & Roskam, J. (2003). *Airplane Aerodynamics and Performance*. DAR Corp.
5. Sadraey, M. (2009). *Aircraft Performance Analysis*. VDM Verlag Dr. Müller.
6. Anderson, J. D. (1999). *Aircraft Performance and Design*. McGraw-Hill.
7. Roskam, J. (2007). *Airplane Flight Dynamics and Automatic Flight Control*, Part I. DAR Corp.
8. Etkin, B., & Reid, L. D. (1996). *Dynamics of Flight, Stability and Control*. Third Edition, Wiley.
9. Stevens, B. L., & Lewis, F. L. (2003). *Aircraft Control and Simulation*. Second Edition, Wiley.
10. Chemezov, D., et al. (2021). Pressure distribution on the surfaces of the NACA 0012 airfoil under conditions of changing the angle of attack. *ISJ Theoretical & Applied Science*, 10 (101), 601-606.
11. Chemezov, D., et al. (2021). Stressed state of surfaces of the NACA 0012 airfoil at high angles of attack. *ISJ Theoretical & Applied Science*, 10 (102), 601-604.
12. Chemezov, D., et al. (2021). Reference data of pressure distribution on the surfaces of airfoils having the names beginning with the letter A (the first part). *ISJ Theoretical & Applied Science*, 10 (102), 943-958.
13. Chemezov, D., et al. (2021). Reference data of pressure distribution on the surfaces of airfoils having the names beginning with the letter A (the second part). *ISJ Theoretical & Applied Science*, 11 (103), 656-675.
14. Chemezov, D., et al. (2021). Reference data of pressure distribution on the surfaces of airfoils having the names beginning with the letter B. *ISJ Theoretical & Applied Science*, 11 (103), 1001-1076.
15. Chemezov, D., et al. (2021). Reference data of pressure distribution on the surfaces of airfoils having the names beginning with the letter C. *ISJ Theoretical & Applied Science*, 12 (104), 814-844.
16. Chemezov, D., et al. (2021). Reference data of pressure distribution on the surfaces of airfoils having the names beginning with the letter D. *ISJ Theoretical & Applied Science*, 12 (104), 1244-1274.
17. Chemezov, D., et al. (2022). Reference data of pressure distribution on the surfaces of airfoils (hydrofoils) having the names beginning with the letter E (the first part). *ISJ Theoretical & Applied Science*, 01 (105), 501-569.
18. Chemezov, D., et al. (2022). Reference data of pressure distribution on the surfaces of airfoils (hydrofoils) having the names beginning with the letter E (the second part). *ISJ Theoretical & Applied Science*, 01 (105), 601-671.